J. Eukaryot. Microbiol., 53(6), 2006 pp. 464–476

DOI: 10.1111/j.1550-7408.2006.00139.x

Trachipleistophora extenrec n. sp. a New Microsporidian (Fungi: Microsporidia) Infecting Mammals

JIŘÍ VÁVRA,[a,b] ALEŠ HORÁK,[a,b] DAVID MODRÝ,[a,c] JULIUS LUKEŠ[a,b] and BŘETISLAV KOUDELA[a,c]

[a]*Institute of Parasitology, Biological Centre of the Czech Academy of Sciences, České Budějovice, and*
[b]*Faculty of Biology, University of South Bohemia, České Budějovice, and*
[c]*Department of Parasitology, University of Veterinary and Pharmaceutical Sciences, Brno, Czech Republic*

ABSTRACT. A new microsporidian *Trachipleistophora extenrec* n. sp. was isolated from a muscle lesion of the streaked tenrec *Hemicentetes semispinosus* Cuvier, 1798 (Mammalia, Tenrecidae), an insectivore endemic to Madagascar. The spores isolated from the tenrec were infectious to severe combined immunodeficient (SCID) mice by intramuscular injection. Material obtained from muscular lesions in mice was used for the parasite description. All developmental stages of the microsporidian were covered by a dense coat, which during sporogony changed into the sporophorous vesicle wall. Eight, 16, 32, or more spores were formed inside the sporophorous vesicle as the result of the division by plasmotomy and sequential fission of a multinucleate sporogonial plasmodium. Spores were ovoid, 4.7 × 2.8 μm in size, had a large posterior vacuole, and had an isofilar polar tube with 15–16 coils. Although the fine structure and the developmental pattern of the organism were in some respects similar to the genus *Vavraia*, molecular phylogeny based on the gene sequences of the small subunit rRNA and RNA polymerase subunit II indicated that the organism belongs to the genus *Trachipleistophora*. The diagnostic characters of the genera *Trachipleistophora* and *Vavraia* are discussed as well as the discrepancies between the phylogenies of these two microsporidian genera based on morphology and molecules.

Key Words. Insectivora, microsporidia, molecular phylogeny, muscle tissue, RPB1 gene, Tenrecidae, ultrastructure, *Vavraia*.

MICROSPORIDIA, now considered to be fungi or their relatives (Fast, Logsdon, and Doolittle 1999; Hirt et al. 1999; Keeling, Luker, and Palmer 2000), are among the most common parasites of animals with more than 1,200 species described in about 130 genera. However, the number of species recorded in mammals, including man, is relatively low (Canning and Lom 1986; Didier et al. 2000; Mathis, Weber, and Deplazes 2005). Two groups of mammalian microsporidia can be distinguished: (1) species using mammals as their true hosts (i.e. *Encephalitozoon* and *Enterocytozoon*), and (2) a group of ''opportunistic microsporidia,'' evidently having some other hosts than mammals, but able to infect mammals accidentally (i.e. *Brachiola, Vittaforma, Trachipleistophora*, *Pleistophora*, and several poorly described species) (Mathis et al. 2005).

Immunoprivileged sites, such as the mammalian eye, or immunodeficient status are apparently the prerequisites for patent opportunistic microsporidian infections in mammals. Therefore, several microsporidia, some of them not well defined, are known to cause eye infections (Mathis et al. 2005) and, as shown experimentally, the eye can serve as an effective portal of entry for these parasites into the mammalian body (Koudela, Vávra, and Canning 2004; Koudela et al. 2001). Other opportunistic microsporidia reside in skin, muscles, or even cause systemic infections (Cali and Takvorian 2003; Mathis et al. 2005; Vávra et al. 1998). Such microsporidia should be able to withstand the body temperature of the homoiothermic organism and should be able to successfully survive within mammalian cells (Koudela et al. 2004). It is not known how many microsporidia possess these two prerequisites. This is certainly not their general quality as documented by the unsuccessful attempts to infect mammals with insect or fish microsporidia (Cheney, Lafranchi-Tristem, and Canning 2000) or to grow insect microsporidia in mammalian cell culture (Wang 1982 cited in Becnel, White, and Shapiro 2005). As the incidence of immunodeficiency in the human population is rising from HIV infections, post-transplantation treatments, and genetic causes, it is of general interest to explore microsporidia able to infect mammals. The present paper describes a novel opportunistic microsporidian species able to infect and complete its life cycle within the mammalian host.

MATERIALS AND METHODS

Parasite isolation. The streaked tenrec *Hemicentetes semispinosus* Cuvier, 1798 infected with the microsporidian described in the present paper was found in a group of 20 animals caught in Madagascar and shipped to the Czech Republic for commercial purposes. The imported animals were admitted to the Department of Parasitology, University of Veterinary and Pharmaceutical Sciences, Brno, Czech Republic, for parasitological examination. Some tenrecs were extremely emaciated and were therefore euthanized and necropsied. In one of the necropsied animals, microscopical examination of the diaphragm muscle revealed the presence of structures suggesting muscular microsporidiosis. Subsequently, a part of the diaphragm muscle was homogenized in sterile phosphate buffered solution (PBS) and the diagnosis was verified by staining the microsporidian spores with the optical brightener Calcofluor White 2MR (Vávra et al. 1993).

The remaining diaphragm muscle of the necropsied tenrec was homogenised in sterile PBS supplemented with antibiotics and the suspension containing microsporidian spores was injected into the gluteal muscle of a SCID mouse. This inoculated SCID mouse was euthanized and necropsied at day 95 postinfection and its tissues were examined for the presence of microsporidia. The leg muscles containing microsporidian spores were excised, homogenised in sterile PBS, and incubated with 0.25% (w/v) trypsin for 20 min at 37 °C. The spore suspension was centrifuged and resuspended in PBS. Spores were then purified by centrifugation at 1,000 *g* for 15 min, and layered on top of the column of 50% Percoll in PBS. After washing and resuspension in sterile PBS, the spores were counted using a haemocytometer, and adjusted to the required concentration.

Light microscopy. Standard histology methods, including paraffin sections stained by hematoxylin–eosin and Gram's method, were used for the examination of the infected SCID mouse. Spore size and shape were recorded by photography and morphometry (Vávra and Maddox 1976). Spores were also measured from samples digitally projected on a computer screen.

Electron microscopy. For transmission electron microscopy (TEM), tissue samples from the site where spores had been inoculated into the SCID mouse were fixed in 2.5% (v/v)

Corresponding Author: B. Koudela, Department of Parasitology, University of Veterinary and Pharmaceutical Sciences, Palackého 1-3, 612 42 Brno, Czech Republic—Telephone number: +420-5-41562262; FAX number: +420-5-41562266; e-mail: koudelab@vfu.cz

glutaraldehyde in 0.1 M cacodylate buffer (pH 7.4) at 4 °C and postfixed in 1% (w/v) osmium tetroxide in the same buffer. Tissue samples were then washed in the same cacodylate buffer, dehydrated in a graded ethanol series, and embedded in Durcupan epoxy resin. Ultrathin sections were stained with uranyl acetate and lead citrate and examined in a JEOL 1010 electron microscope equipped with a Megaview 3 CD camera. Electron micrographs of *Vavraia culicis* (Weiser 1977) and *Trachipleistophora hominis* (Hollister et al. 1996) served for comparison. Spores of *V. culicis* (Florida isolate), kindly provided by James Becnel (USDA/ARS CMAVE, Gainesville, FL, USA), were used to infect *Spodoptera exigua* larvae, which were subsequently prepared for electron microscopy as described above. The origin and handling of *T. hominis* was as described previously (Koudela et al. 2004).

DNA isolation, PCR, and sequencing. Total DNA was isolated from pieces of heavily infected tissue using standard phenol–chloroform extraction (Maslov et al. 1996). The small subunit (SSU) rRNA gene was amplified from about 20 ng of genomic DNA using primers 18f (5′- CACCAGGTTGATTCTGCC -3′) and 1492 (5′-GGTCCAGCAGCCGCGG-3′) and 1U of Taq Purple polymerase (Top-Bio, Prague, Czech Republic). The reaction conditions were as follows: 95 °C for 5 min, followed by 30 cycles at 95 °C for 1 min, 55 °C for 1 min, and 72 °C for 1 min, with a final extension of 5 min at 72 °C. The D-F region of the RNA polymerase subunit II (RPB1) gene was amplified using partly degenerate primers RNApF1 (5′-GTGCTGTCGTGCCAGGGYAACAAGC-3′) and RNApR1 (5′-GTCGATGCATCCCTTGATGAGTATGC-3′) and with the use of above-described PCR programme. The amplicons of expected size were gel purified using the Jetquick gel extraction kit (Genomed™, Löhne, Germany) and cloned into the Topo TA cloning vector (Invitrogen™, Carlsbad, CA, USA). Both strands were sequenced

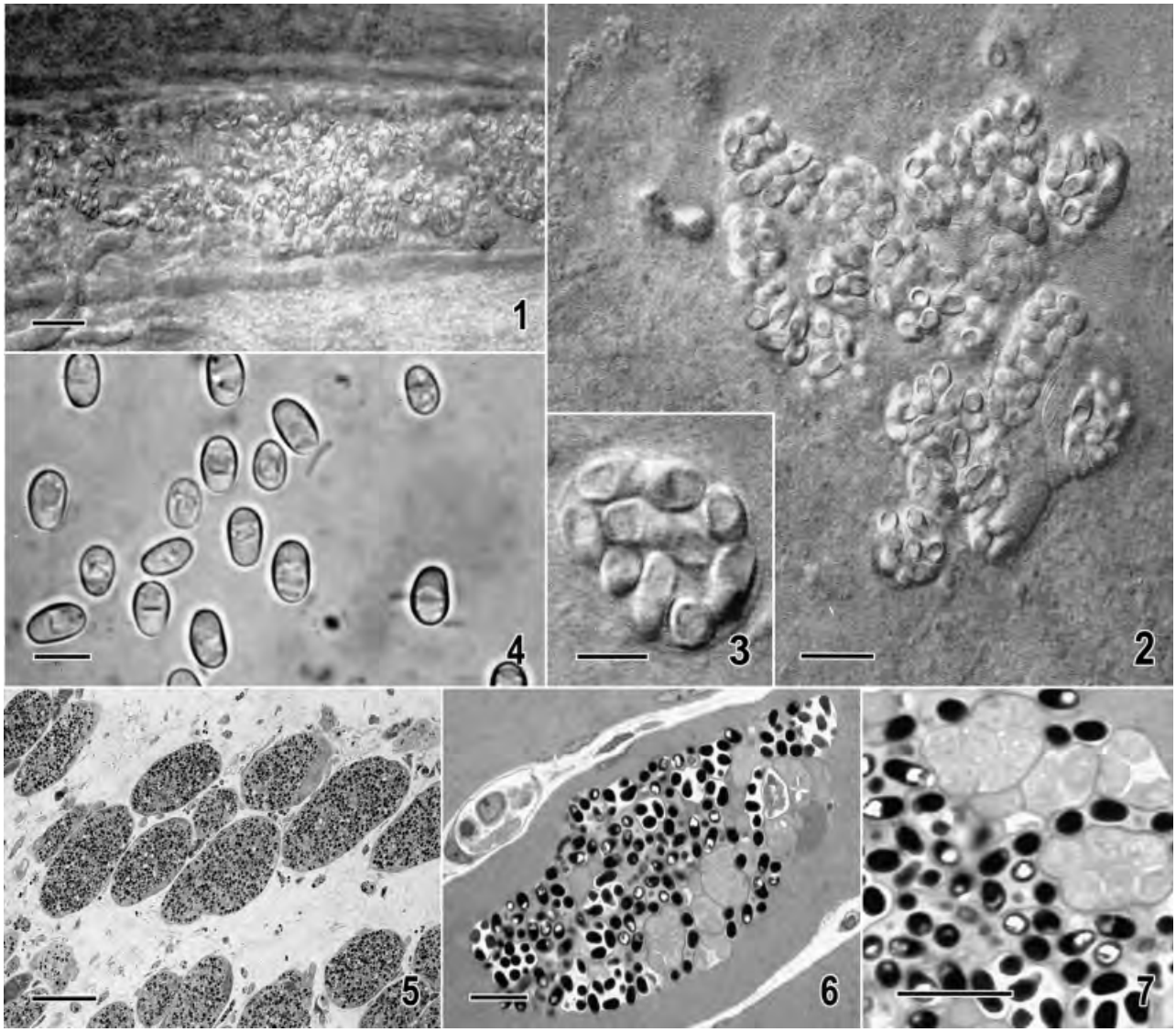

Fig. **1–7.** *Trachipleistophora extenrec* n. sp. in muscles of the tenrec *Hemicentes semispinosus*. Fig. **1.** Muscle fiber filled with sporophorous vesicles and spores (Bar = 20 μm). Fig. **2.** A mass of sporophorous vesicles with spores (Bar = 10 μm). Fig. **3.** Individual sporophorous vesicle (Bar = 5 μm). *Trachipleistophora extenrec* n. sp. from muscles of an infected severe combined immunodeficient (SCID) mouse. Fig. **4.** Fresh isolated spores. Note the large posterior vacuole and the slight asymmetry of the spore shape (Bar = 5 μm). Fig. **5–7.** Semithin sections, toluidine blue staining. Fig. **5.** Infected muscle fibers at low magnification (Bar = 50 μm). Fig. **6.** Muscular lesion at higher magnification. Note that the muscle around the lesion is not altered (Bar = 20 μm). Fig. **7.** Developmental stages among ripe spores (Bar = 20 μm).

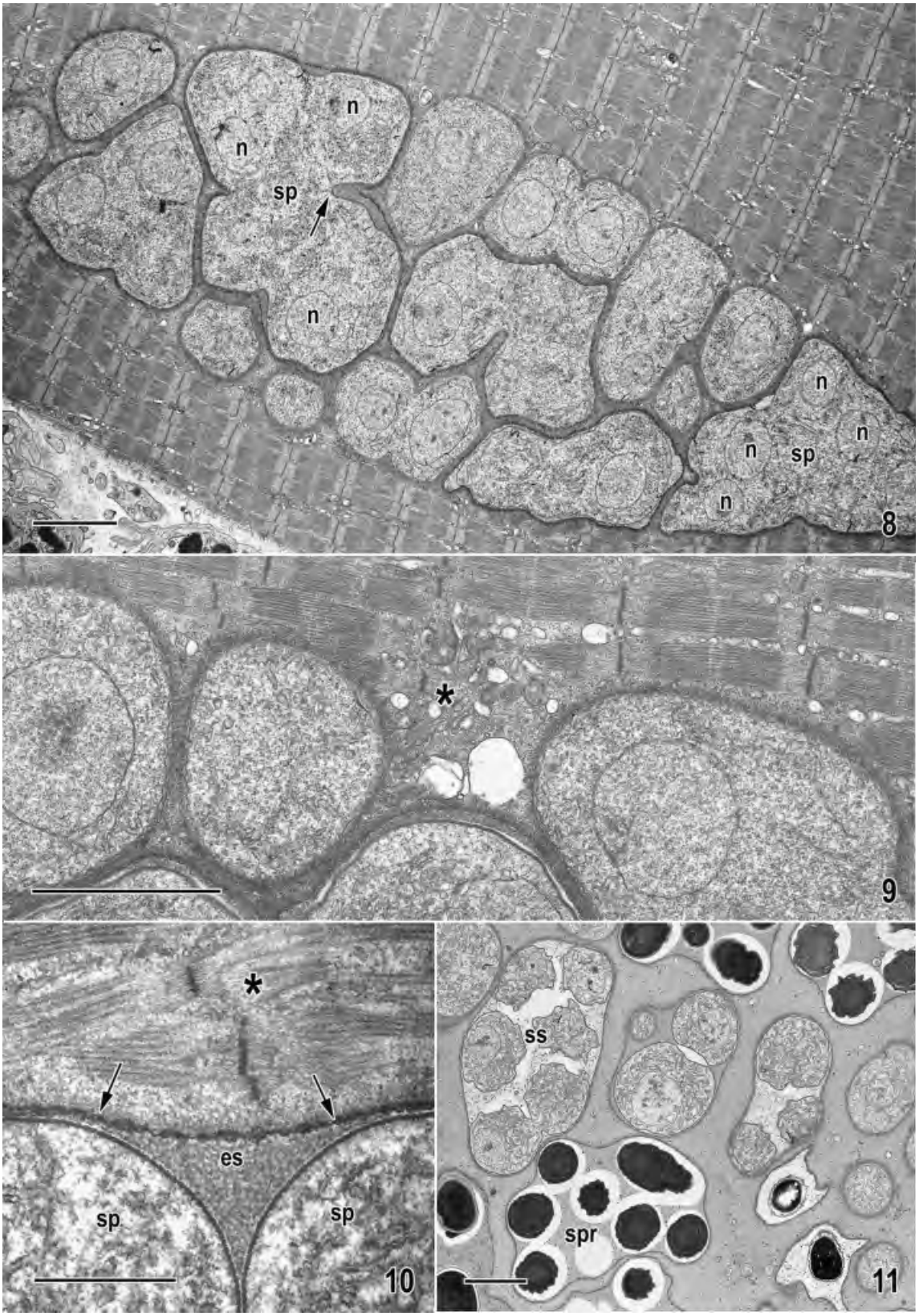

Fig. **8–11.** Electron microscopy of *Trachipleistophora extenrec* n. sp. in an infected severe combined immunodeficient (SCID) mouse, host–parasite relationship. Fig. **8.** Late meronts and early sporonts (sp) with several nuclei (n) are located in nearly intact muscle, the parasites being separated by channels of host and parasite materials. Cell division involves deep infolding of the cell surface including the cell coat (arrow) (Bar = 2 μm). Fig. **9.** Close to the parasite the myofibrils are dissolved into a vesicular mass (*) (Bar = 2 μm). Fig. **10.** In some places the myofibrils are frayed (*). Sporophorous vesicle wall is at arrow: sp, sporonts; es, episporontal space (Bar = 500 nm). Fig. **11.** In advanced lesions containing advanced sporogonial stages (ss) or sporophorous vesicles with spores (spr), the host tissue is replaced by nearly structureless material (Bar = 1 μm).

on an automatic sequencer (Beckman Coulter, Fullerton, CA, USA) and sequence fragments were completed with Editseq and Seqman (DNAStar, Madison, WI, USA).

Phylogenetic analysis. The SSU rRNA sequence was aligned with the following microsporidian sequences retrieved from the Genbank: *Tetramicra brevifilum* (AF364303), *Glugea anomala* (AF044391), *Glugea atherinae* (U15987), *Loma acerinae* (AJ252951), *Trachipleistophora hominis* (AJ002605), *Vavraia culicis* (AJ252961), *Vavraia oncoperae* (X74112), *Pleistophora mirandellae* (AJ252954), *Pleistophora ovariae* (AJ252955), *Pleistophora typicalis* (AJ252956), *Ovipleistophora mirandellae* (AF356223), *Heterosporis anguillarum* (AF387331), *Heterosporis* sp. PF (AF356225), and *Pleistophora* sp. 3 (AF044390). Multiple alignments of different transitions/transversions (Ts/Tv) ratios were created (1:1, 1:2, 1:3, and 1:5) and further edited using the mCLUSTAL X 1.83 (Thompson et al. 1997). Ambiguously aligned regions and gaps were removed using BioEdit 7.0.4.1 (Hall 1999) and Gblocks (Castresana 2000) software. The PCR-amplified D-F region of the RPB1 gene was aligned with the homologs from *V. culicis* (AJ278956), *T. hominis* (AJ278945), and *P. typicalis* (AJ278946) and further processed as described above for SSU rRNA.

The SSU rRNA and RBP1 data sets were analyzed by maximum likelihood (ML) under the GTR+G8+I and HKY+G8 models of evolution, respectively, chosen according to the Akaike criterion as implemented in Modeltest 3.7 (Posada and Crandall 1998), with use of Phyml 2.4.4 software (Guindon and Gascuel 2003). Bootstrap support was assessed from 2,000 replications by the ML algorithm and the above-described model and software and by maximum parsimony (MP) using PAUP 4.0b10 (Swofford 2002). Bayesian posterior probabilities (Bayesian inference, BI) were calculated using MrBayes 3.0b4 (Huelsenbeck and Ronquist 2001) under the above-described model with Markov chain set to 4×10^6 generations, every 100th tree sampled, and the first 10^6 generations omitted.

RESULTS

Light microscopy. Examination of the muscular lesion of the tenrec showed muscle fibers filled with microsporidian spores (Fig. 1). At higher magnification, dense clumps of spores were recognized (Fig. 2). Nomarski phase contrast microscopy of smeared parts of the muscular lesion demonstrated the presence of spores possessing a large posterior vacuole and forming packets enveloped by a membrane (Fig. 3). Spores were ovoid and measured 4.7 (4.0–5.0) μm × 2.8 (2.5–2.9) μm (n = 20) when fresh (Fig. 4). Semithin sections of the epoxy resin-embedded material obtained from muscular lesions of the inoculated SCID mouse demonstrated an extensive infection of muscle fibers (Fig. 5). At higher magnification, the foci of spores and developmental stages located in the seemingly intact muscle were observed (Fig. 6, 7).

Electron microscopy. Ultrathin sections of the muscle lesions of the infected SCID mouse showed both early and advanced foci of infection (Fig. 8, 11). In early lesions (i.e. without spores), closely adjacent developmental stages of the parasite occurred (Fig. 8). Higher magnification showed that the muscle fine structure was altered only at the immediate vicinity of the parasite (Fig. 9). The myofibrils were frayed (Fig. 10) and appeared to be replaced by fine granular matrix interspersed with small vesicles (Fig. 9). Similarly looking matrix separated individual stages of the parasite. In no case did two parasite cells adhere to each other: there was always a gap of about 340–370 nm containing a medium density matrix separating them. Thus, the whole lesion was in fact permeated by a network of channels (Fig. 8). In advanced sporogony lesions (i.e. in those already containing spores), the sporophorous vesicles (SPOV) with sporogonial stages or spores were more dispersed in a structureless matrix of transformed host tissue (Fig. 11).

Close inspection of lesions at different stage of development revealed the existence of the following respective life cycle stages in tissues of the SCID mouse inoculated with the microsporidian: early meronts (m1), meronts of different maturation stage (m2, m3), early sporonts (s1), late sporonts (s2), sporoblasts, and spores. Cytoplasm density and structure, plasmalemma appearance, and coat structure were the respective distinguishing characters.

The m1 meronts, representing cells probably grown from sporoplasms, were found only once. They were represented by cells (2.5–3.0 μm in size) with one or two separate nuclei and a cytoplasm with ribosomes, which were less abundant than in the typical m2 and m3 meronts. Cisternae of the endoplasmic reticulum (ER) were absent and the cytoplasm contained only some ill-defined vacuoles. Frequently, there was a slit separating part of the two membranes wrapping up the nucleus (Fig. 12). The m1 meronts were surrounded by plasma membrane covered from the outside by a 30–40 nm double-layer coat consisting of a less dense material adhering to the thickened plasmalemma with a diffuse line of dense layer material on top (Fig. 13).

The m2 meronts were also rare in our material and were represented by round cells (3.0 μm in diam.) with one or two separate nuclei, very dense cytoplasm with numerous ribosomes, very few ER cisternae, and no Golgi vesicles (Fig. 14). These stages were surrounded by a coat similar to that of m1 meronts except that the outside dense layer had a more diffuse aspect (Fig. 15).

In m3 meronts, the general aspect of the cytoplasm was similar to m2 meronts. However, the cytoplasm was somewhat less dense as it contained small and diffuse transparent spots, representing probably future ER (Fig. 16). The cell coat of m3 meronts was around 90–100 nm thick and was constituted of a dark layer on the outer leaf of the plasmalemma protruding as numerous finger-like curls into a layer of diffuse dense material (Fig. 17, 18). The curls were bordered by a very thin lucent layer and a thin layer of diffuse dense material on top of it (Fig. 18). On one occasion, a group of meronts probably just ready for transformation into sporonts, as judged from their transparent cytoplasm, was found in a lysed host cell. These meronts contained a nearly continuous membranous layer, bordering the dark layer of the parasite's cell coat (Fig. 19, 20).

The next developmental stages, identified as early sporonts (s1) were abundant and represented the main proliferative form of the parasite inside the muscle lesions. They were cells with transparent cytoplasm, clearly showing several ER cisternae. Vesicular accumulations characteristic for the microsporidian Golgi apparatus were absent. The cells had one to several nuclei and were often found in the process of division (Fig. 8, 21). Their coat was very indistinct at this stage and it was difficult to distinguish the coat material from the matrix separating individual parasite cells inside the lesion. The coat was interpreted as being about 60 nm thick and consisting of a patchily thickened plasma membrane outer leaf, a less dense intermediate layer filled with finely granular material, and a thin, dense membrane-like layer aligned externally. The outer thin membrane-like layer formed numerous tubular protrusions into the matrix separating individual parasite cells (Fig. 22, 23). During fission of these stages, the plasma membrane and its coat invaginated deeply into the cell, finally separating the daughter cells (Fig. 8, 21).

Advanced sporonts (s2) were multinucleate cells similar to s1 sporonts in which, however, the extracellular coat started to detach from the thickened plasma membrane (Fig. 24, 25). This process actually led to the transformation of the sporont coat into a SPOV wall, which finally enclosed the division products of the sporogonial plasmodium (Fig. 11, 26). During the final stage of

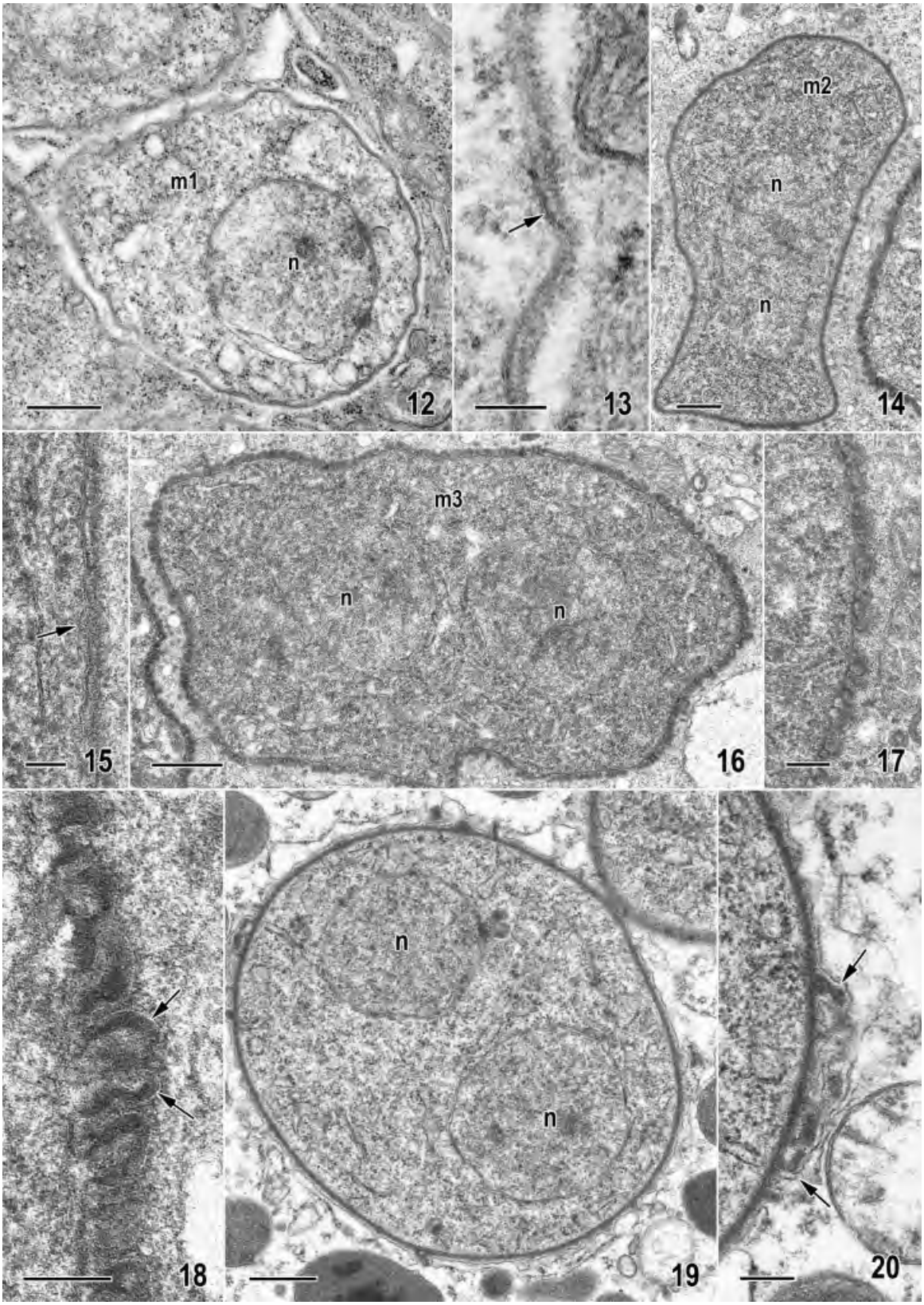
m1
n
12
13
m2
n
n
14
15
m3
n
n
16
17
18
n
n
19
20

sporogony, the plasmalemma became thickened by dense material and the coat layer was changed into a dense undulating bilayer about 50 nm thick. This structure was composed of a very dense inner layer (20 nm), a transparent inner layer (25 nm), and an outside thin dense layer (5 nm), all layers being aligned with each other in their undulating course (Fig. 25; inset). There was a fine granular material of medium density in the space between the now detached plasmalemma and the coat (termed the episporontal space; es). While the retraction of the late sporont plasma membrane from the coat continued, successive divisions led to s2 cells with fewer nuclei and finally to uninucleate sporoblasts (Fig. 11). This division was first by plasmotomy and later by binary fission. The material in the episporontal space started to disappear in areas close to the dividing cells (Fig. 11) and disappeared in the course of development (Fig. 26).The sporoblasts were extremely dense cells of irregular outline with no discernible internal substructure (Fig. 26).

Sporoblasts and spores were enclosed in SPOVs represented by an about 50 nm thick, undulating layer of dense material contoured by a line of less dense amorphous material and separated from the basal layer by a gap (Fig. 27, 28). In tangential sections, the SPOV was revealed as a maze of both above-mentioned materials, providing the enormous surface area in which the parasite communicated with the host cell (Fig. 29). Young spores had the polar filament coils lesser in number and arranged in a single row (Fig. 11, 27). Mature spores were surrounded by a 70 nm thick, lucent endospore and a thinner exospore (45 nm) (Fig. 30–32). The endospore was thinned to about 25 nm in the region above the anchoring disc. In some electron micrographs, the exospore looked like a single layer of medium density, bordered on the outside by a thin dense line (Fig. 30, 32). Elsewhere, however, a more complex exospore construction was visible. The following layers were discerned in the direction from the endospore toward the spore surface: (1) a 25-nm layer of medium density; (2) a 5-nm very dense layer; (3) a 10-nm layer of medium density; and (4) a 5-nm layer of very high density (Fig. 34).

The polar filament was anchored subapically, had a prominent polar sac, and had 15–16 isofilar coils arranged as 10–11 coils in one row aligned with the spore wall and another four to five coils forming a second line located more internally (Fig. 32). In cross-section, the coils measured about 115 nm and showed several rings of material of varying density (Fig. 33). The typical polaroplast was composed of membranous lamellae closely stacked anteriorly and less closely stacked posteriorly (Fig. 30, 31).

Phylogenetic analysis. The SSU rRNA sequence was aligned with 14 microsporidian SSU rRNA genes obtained from the GenBank™, generating a 1,147-bp-long alignment containing 197 parsimony-informative positions. Based on the previous analyses with more general taxon sampling (data not shown) the dataset was rooted with *T. brevifilum*. All three methods in combination with all Ts:Tv weights (i.e. a total 12 analyses) revealed a similar topology (Fig. 39). Very robustly supported terminal nodes are branched together with support decreasing to the basal nodes.

All species split into three main clades, the first one being composed of both *Glugea* species and *Loma acerinae*. The second clade comprised *Heterospora* spp., *Pleistophora ovariae*, *P. mirandellae*, and *Ovipleistophora mirandellae*. The third clade contained members of the genera *Pleistophora*, *Vavraia*, and *Trachipleistophora*, including the newly described species. In MP, ML, and BI analyses, the SSU rRNA sequence of *T. extenrec* sp. n. was most closely related to *T. hominis*, with both *Vavraia* species constituting a closely related sister group. It should be noted that in the *Trachipleistophora-Vavraia* clade all branches are rather short. The topology was stable and very robust in all analyses performed (Fig. 39).

The conflict in the generic assignment based on the ultrastructural and SSU rDNA data prompted us to explore the informative value of the RPB1 gene, in particular its D-F region (Cheney et al. 2001). Due to high variability, this $\sim$ 600-bp-long region was unambiguously alignable only in its 5′ and 3′ regions. Since a close relatedness with the genera *Trachipleistophora* and *Vavraia* was established in the SSU rRNA-based trees, we have narrowed the RPB1 alignment to only these two genera with *P. typicalis* being used as an outgroup (Fig. 40). Simple evaluation of this alignment by eye reveals that in the D-F region, *T. extenrec* n. sp. shares unique insertions with *T. hominis*, although both species significantly differ in the sequence of the hypervariable regions. Phylogenetic analyses of this alignment using ML, MP, and BI unambiguously supported a common origin of both species (Fig. 39). In this respect the 16-bp-long insertion between nucleotides 562 and 563 of the RPB1 gene, shared between *T. extenrec* n. sp. and *T. hominis*, but absent in *Vavraia* and *Pleistophora*, appears to be most characteristic for the genus *Trachipleistophora* (Fig. 40).

DISCUSSION

The source of infection for the tenrec remains enigmatic and one can only speculate that the emaciated state of the animal together with the stress involved in capture and shipping helped the microsporidian to establish itself in the host. A hypothesis that the insectivorous tenrec acquired the infection from its food should be considered. While the source of infection remains unknown, both the structural, host, and molecular characters of the described organism confirm its identity as a new species (Table 1).

As the meronts had on their plasmalemma an external layer that was later transformed into the wall of the SPOV, the parasite undoubtedly belongs among microsporidia forming the so-called merontogenetic sporophorous vesicle (Vávra and Larsson 1999). Three microsporidian genera, namely *Pleistophora, Trachipleistophora*, and *Vavraia* are known to share this feature. A close relationship of the described microsporidian with the genus *Pleistophora* was excluded, as meronts of this genus are surround-

Fig. **12–20.** Electron microscopy of *Trachipleistophora extenrec* n. sp. in an infected severe combined immunodeficient (SCID) mouse, merogonial stages. Fig. **12.** An early (m1) uninucleate (n) meront. The cytoplasm has vacuolate character, contains ribosomes but no ER or Golgi vesicles (Bar = 500 nm). Fig. **13.** Detailed view of Fig. 12, showing the cell coat consisting of a diffuse layer of material, separated from the thickened plasmalemma (arrow) by a gap (Bar = 100 nm). Fig. **14.** Older (m2) meront has dense nuclei (n) and a very dark cytoplasm with numerous ribosomes, few ER cisternae and no Golgi vesicles (Bar = 200 nm). Fig. **15.** Detail of Fig. 14. The plasmalemma (arrow) is covered by a 30- nm coat consisting of a 10- nm thick innermost electron-lucent layer and a 20- nm thick layer of diffuse dense material (Bar = 100 nm). Fig. **16.** A binucleate older (m3) meront (n = nuclei) close to the transformation into a sporont. The cytoplasm has slightly less dense aspect due to the appearance of electron-lucent vacuolar spots, with the cell coat being thicker (100 nm) and more complex (Bar = 500 nm). Fig. **17** shows a detail of Fig. 16. Dark material on the plasmalemma forms curling extension into a structureless fuzzy material (Bar = 200 nm). Fig. **18.** Detail of the cell coat of a meront close to the change into a sporont. Dark material forming the curls is separated from the extracellular milieu by a thin, membranous layer (arrows) (Bar = 100 nm). Fig. **19.** Binucleate (n) meront approaching the sporont stage and situated in a lysed host cell (Bar = 500 nm). Fig. **20.** Detail of the cell coat of the meront in Fig. 19. Note expansions of the dark coat material into the host cell cytoplasm, which are limited from the outside by a thin membrane-like layer (arrows) (Bar = 200 nm).

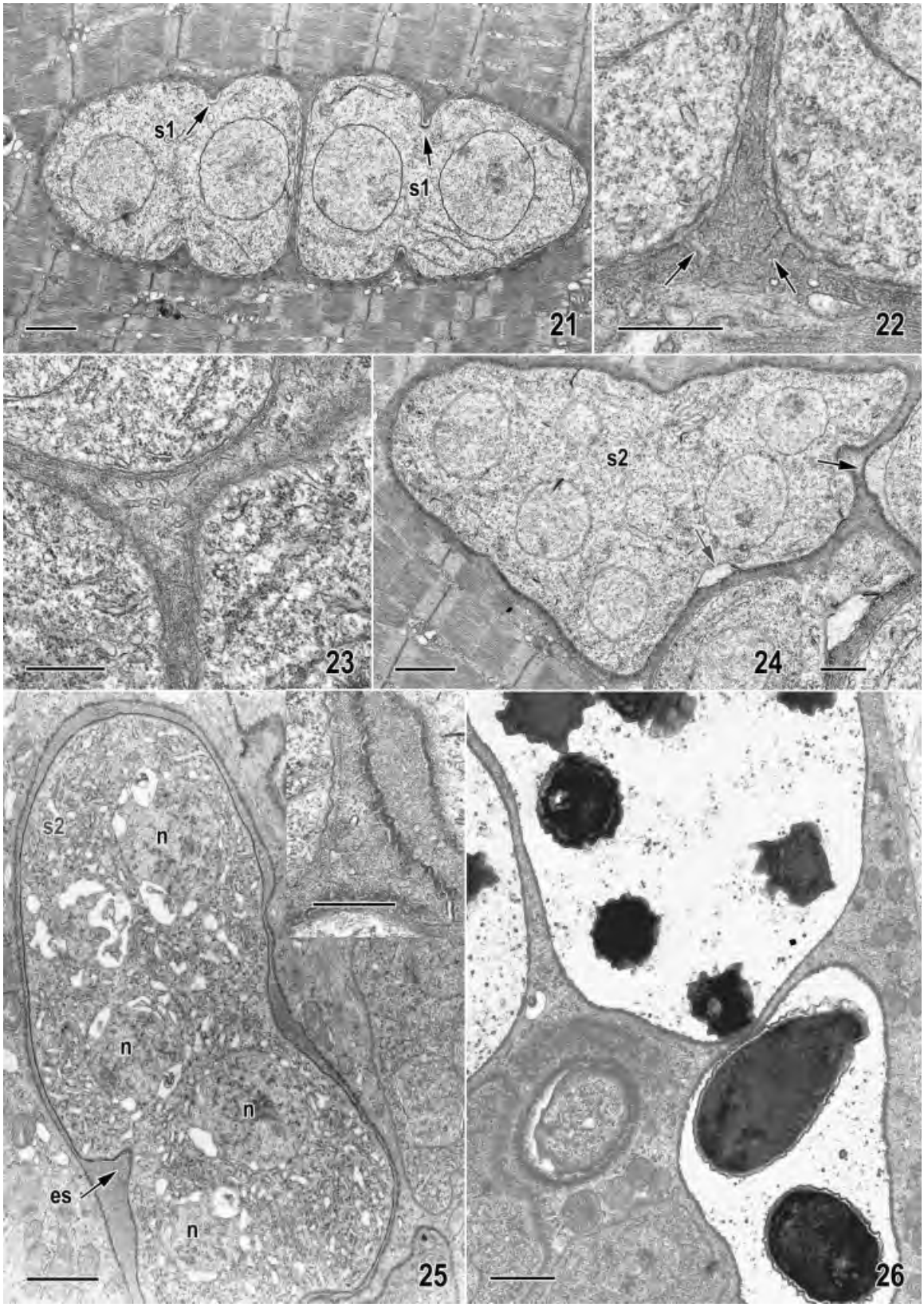
s1
s1
21
22
23
s2
24
s2
n
n
n
n
es
25
26

ed by a thick layer of amorphous material, permeated by vesicles (Canning and Hazard 1982; Canning, Killick-Kendrick, and Killick-Kendrick 1991; Lom and Nilsen 2003). To decide whether the species described herein belongs to the genus *Vavraia* or *Trachipleistophora* proved, however, difficult if only morphological characters were considered. These genera are morphologically quite similar and they are also closely related in trees based on the SSU rRNA (Cheney et al. 2000) and large subunit of the RPB1 gene sequences (Cheney et al. 2001). The genera *Vavraia* and *Trachipleistophora* share the following characters: (1) nuclei are unpaired throughout merogony and sporogony; (2) meronts are surrounded by a plasmalemma and a thin coat layer of amorphous material secreted externally; and (3) meiosis was not observed. After the plasma membrane of the sporont retracted, the coat transforms into the sporophorous vesicle wall. Eight, 16, 32, or a larger number of spores are formed in the sporophorous vesicle (Canning and Vávra 2000). The main character used to distinguish these two genera is structural: *Vavraia* forms multinucleate sporogonial plasmodia dividing into sporoblasts by plasmotomy, while the sporont in *Trachipleistophora* is a uninucleate cell that gives rise to sporoblasts and spores by successive binary fissions.

Based on the above description, *T. extenrec* n. sp. structurally resembled the genus *Vavraia* as characterized by Canning and Hazard (1982) and redefined by Diarra and Toguebaye (1991). However, both available sequences favour its relationship to *T. hominis*, the type species of the genus *Trachipleistophora* and the only representative for which molecular data are available. Our decision to include the described organism into this genus is based on three facts. Detailed re-examination of electron micrographs used in a previous study (Koudela et al. 2004) showed that *T. hominis* also forms, although rarely, multinucleate sporogonial plasmodia (Fig. 35). This questioned the reliability of the sporont nuclear state to distinguish between *Trachipleistophora* and *Vavraia*. The structures of the cell coat and of the SPOV in the described microsporidian were more similar to those of *Trachipleistophora* than to those of *Vavraia*. In *T. hominis*, the dense coat on the plasma membrane and its numerous expansions are contoured by a very thin dense line separated from the coat by a small gap (Fig. 36 and photomicrographs in the paper by Weidner, Canning, and Hollister 1997). In *T. extenrec* n. sp., the coat expansions were rare and the borderline also occurred on the coat, although it was less distinct (Fig. 20). The cell coat of *Vavraia* spp. is represented by a single layer of dense material without outside bordering (Fig. 37, 38). The third, and in our view the most compelling reason for affiliating the described microsporidian with the genus *Trachipleistophora* rather than *Vavraia* is based on the sequence data.

Phylogenetic analysis of the SSU rRNA gene confirmed close relationships of the species in question with the genera *Trachipleistophora* and *Vavraia*. Moreover, analysis of this gene returned the genus *Pleistophora* as a paraphyletic assembly, corroborating previous results (Vossbrinck and Debrunner-Vossbrinck 2005). Even though the SSU rRNA sequence revealed a strong support for the affiliation of the species in question with the genus *Trachipleistophora*, and in light of the somewhat inconclusive morphological evidence, we also examined the RPB1 gene, in particular to its (hyper) variable region. Phylogenies based on this region were previously shown to be congruent with the SSU rRNA-based trees. However, the RPB1 gene provided better resolution below the genus level (Cheney et al. 2001). Indeed, it proved to be particularly suitable in our case, as it unambiguously assigned *T. extenrec* n. sp. to the genus *Trachipleistophora*. The informative value of several insertions in this gene in other members of the *Pleistophora*, *Vavraia,* and *Trachipleistophora* clade should be examined in order to validate their classification potential. To examine in this respect the third known species of the genus *Trachipleistophora*, namely *T. anthropophthera* should be of special interest, as this microsporidian has two sporulation sequences, two kinds of SPOV, and two spore morphs (Vávra et al. 1998; Juarez et al. 2005). In any case, our study adds weight to the proposed complementary value of the RPB1 gene in inferring relationships among closely related microsporidia.

The difficulty that we have had in assigning *T. extenrec* n. sp. to a genus reflects an increasing problem of microsporidian classification, rooted in conflicts between the morphology- and sequence-based phylogenies. Most clearly is this problem demonstrated in the case of some *Amblyospora* species, the life cycle of which requires the passage from a copepod to a mosquito and which form three developmental morphs, each seemingly belonging to a different genus (Becnel et al. 2005). Only molecular biology is able to demonstrate that these morphs represent different life cycle stages of a single organism (Vossbrinck, Andreadis, and Debrunner-Vossbrinck 1998). This stresses the necesssity to include molecular data in the characterization of newly described organisms and the necessity of a critical interpretation of structural data when new genera and species are proposed. In fact, at present, we do not know which structural characters in microsporidia bear a reliable phylogenetic signal and the search for, and careful evaluation of, such characters remains a major challenge in the classification of microsporidia.

TAXONOMIC SUMMARY

Trachipleistophora extenrec n. sp.
Phylum Microsporidia Balbiani 1882
Class Haplophasea Sprague, Becnel and Hazard 1992
Family Pleistophoridae Doflein 1901
Genus *Trachipleistophora* (Hollister et al. 1996)

Generic diagnosis. With characters of the genus modified by the presence of multinucleate sporogonial plasmodia and the presence of the 16-bp-long insertion between positions 562–563 of the RPBl gene specific for the genus *Trachipleistophora*. Surface coat

Fig. **21–26.** Electron microscopy of *Trachipleistophora extenrec* n. sp. in an infected severe combined immunodeficient (SCID) mouse, sporogonial stages. Fig. **21.** Dividing early sporonts (s1) with a more transparent cytoplasm containing many fewer ribosomal particles than the meronts. Nuclei and the sparse endoplasmic reticulum cisternae are clearly visible. Cell division is by deep infolding of the plasmalemma, cell coat included (arrows) (Bar = 1 μm). Fig. **22.** Detail of Fig. 21 showing the expansions of the external membranous layer of the cell coat (arrows) (Bar = 500 nm). Fig. **23.** High magnification image of muscle lesion area in which three early sporont cells meet. The space among individual parasite cells is filled with granular material into which numerous tubular extensions of the parasite coat protrude (Bar = 500 nm). Fig. **24.** Advanced multinucleate sporont (s2) in which the formation of the sporophorous vesicle by cell coat detachment from the plasmalemma is initiated (arrow). The lobate shape of the sporont indicates that the multinucleate cell is going to divide (Bar = 1 μm). Detail of the area where the future sporophorous vesicle is being formed (inset) (Bar = 200 nm). Fig. **25.** More advanced multinucleate sporont (n, nuclei; es, episporontal space) (Bar = 1 μm). In an inset a high magnification view of the three layers forming the sporophorous vesicle wall at initial sporogony is shown (Bar = 500 nm). Fig. **26.** Advanced sporogony stages showing sporoblasts and young spores inside sporophorous vesicles. Note the disappearance of the secretory material inside the sporophorous vesicle (Bar = 1 μm).

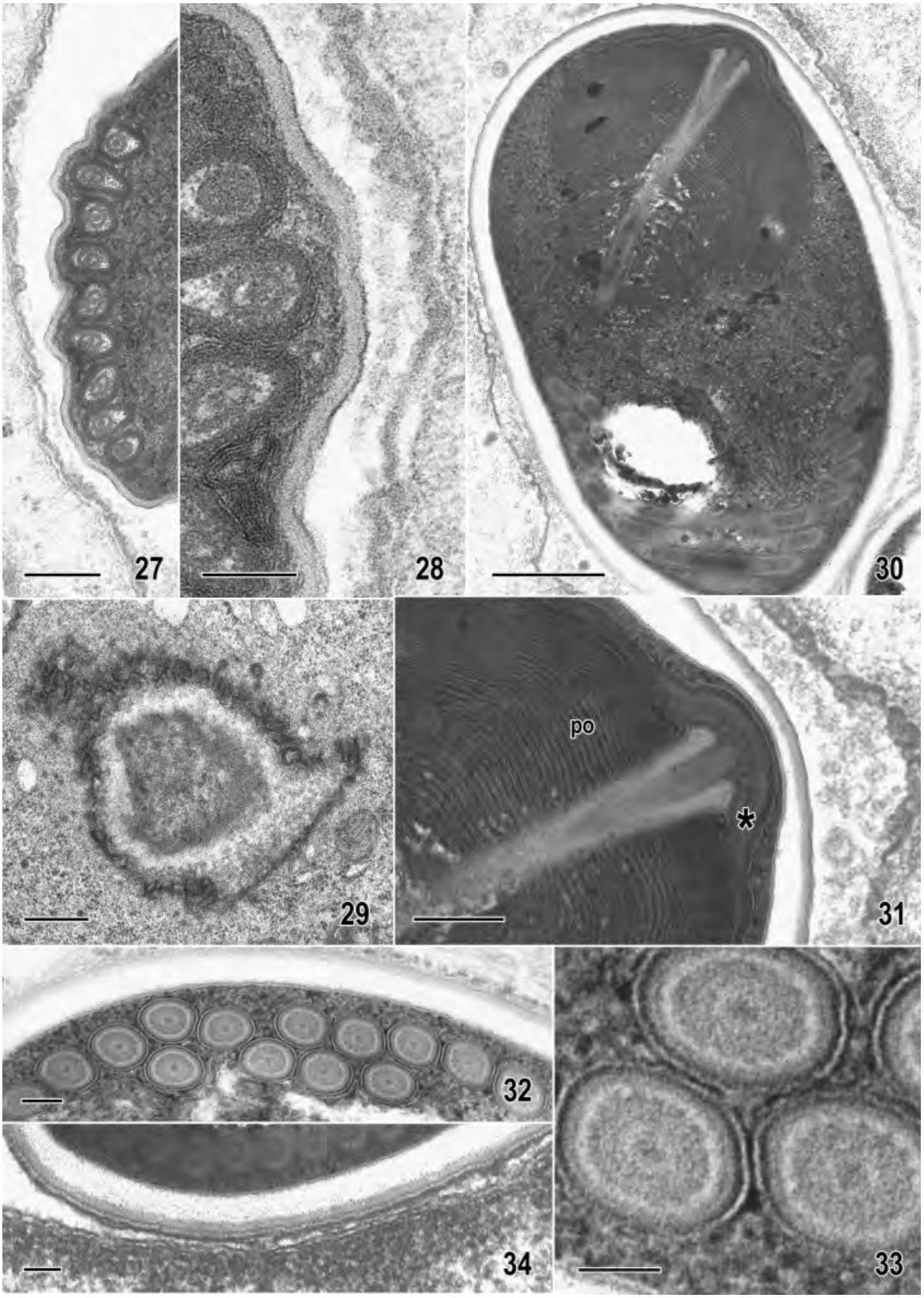
27
28
30
29
po
*
31
32
34
33

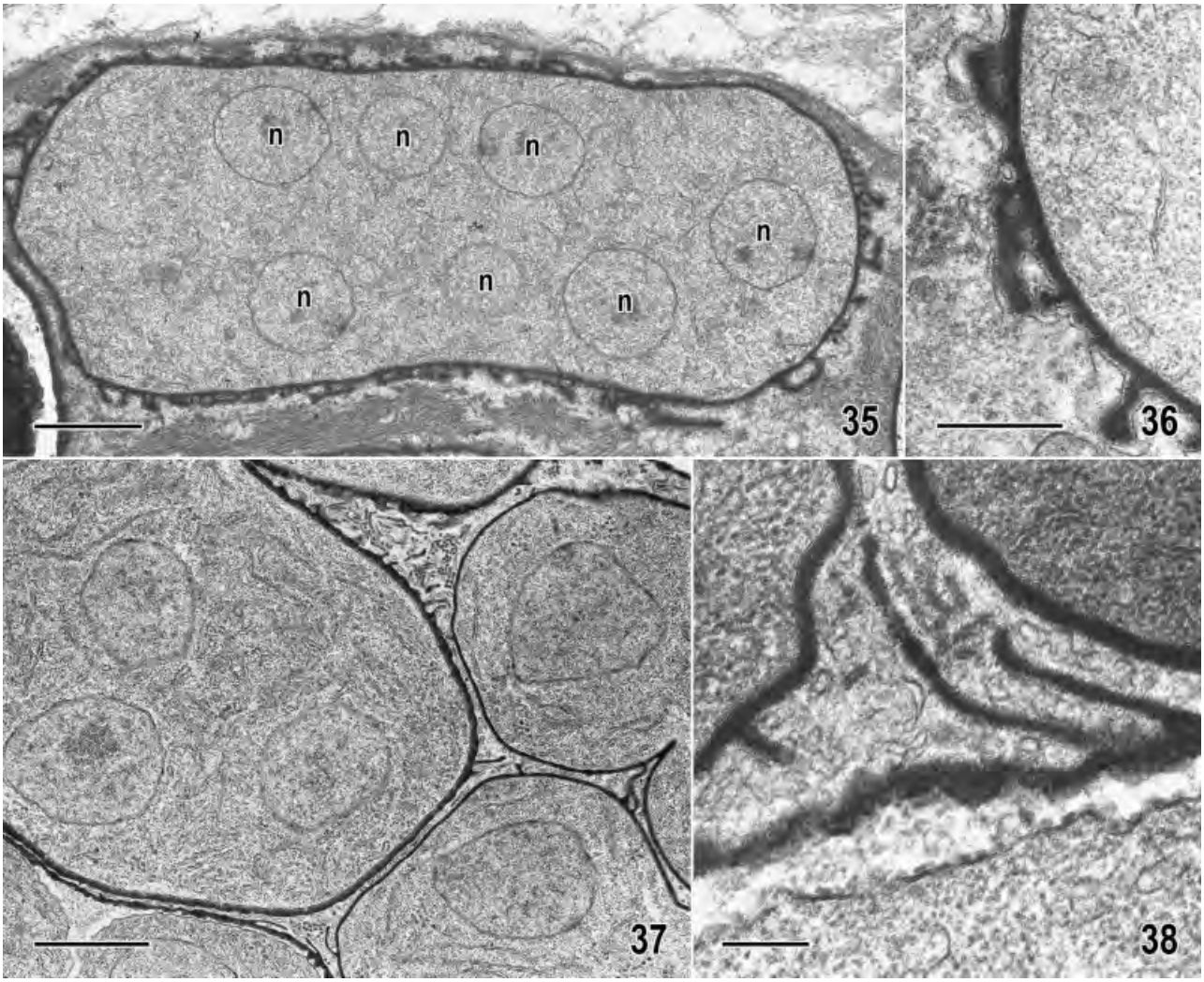

Fig. **35–38.** Electron microscopy of *Trachipleistophora hominis* and *Vavraia culicis*. Fig. **35**, **36.** Electron microscopy of *Trachipleistophora hominis*. Fig. **35.** Multinucleate sporogonial plasmodium (Bar = 1 μm). Fig. **36.** Detailed view of the cell coat construction. Note the thin dark line contouring the expansions of the cell coat (Bar = 500 nm). Fig. **37**, **38.** Electron microscopy of *Vavraia culicis*. Fig. **37.** General view of the cell coat construction (Bar = 1 μm). Fig. **38.** High magnification of the cell coat construction. Note the absence of the line contouring the coat and its expansions (Bar = 200 nm).

on meronts does not form long, anastomosing processes and the coat is not secreted as discoid deposits.

Specific diagnosis. All developmental stages bear a 30–100 nm coat layer on their plasmalemma. The coat later changes into a sporophorous vesicle surrounding a multinucleate sporogonial plasmodium that divides by plasmotomy and binary fission into sporoblasts and spores. Eight, 16, 32, or an irregular number of spores form inside the sporophorous vesicle. Size of spores: 4.7 × 2.8 μm. Number of isofilar coils 14–16, arranged in two parallel rows, a more numerous external row and a less numerous internal row. Polar filament with the diam. 115 nm and composed several concentric layers of material. Anchoring disc subterminal. Polaroplast densely lamellar anteriorly and less compressed posteriorly.

Original host and tissue. *Hemicentetes semispinosus* (Mammalia: Tenrecidae), muscles. Transmissible to *Mus musculus* (Mammalia, Muridae).

Etymology. The specific epithet ''extenrec'' (= ''from tenrec'') reflects the origin of the isolate and is given, in accordance

Fig. **27–34.** Electron microscopy of *Trachipleistophora extenrec* n. sp. in an infected severe combined immunodeficient (SCID) mouse, spore structure. Fig. **27.** Part of a young spore showing that the immature polar filament coils are arranged in one row (Bar = 200 nm). Fig. **28.** The dark, inner undulating material of the sporophorous vesicle is separated by a gap from a thinner layer of an external material; detail of Fig. 27 (Bar = 100 nm). Fig. **29.** Tangential section throughout the mature sporophorous vesicle demonstrating its extensive surface area. Note the association of the dark undulating layer with an electron-dense ill-defined material (Bar = 500 nm). Fig. **30.** Mature spore showing the subapically located anchoring disc, the voluminous polaroplast, thin single-layered exospore and a relatively thick endospore (Bar = 500 nm). Fig. **31.** Detail of the construction of the anchoring disc with the polar sac (*) and the polaroplast (po) with regular membranous lamellae (Bar = 200 nm). Fig. **32.** Mature spore with 14 polar tube coils arranged partly as a single, partly as a double layer (Bar = 100 nm). Fig. **33.** High magnification view of the polar tube (Bar = 50 nm). Fig. **34.** Details of the construction of the spore wall (Bar = 100 nm).

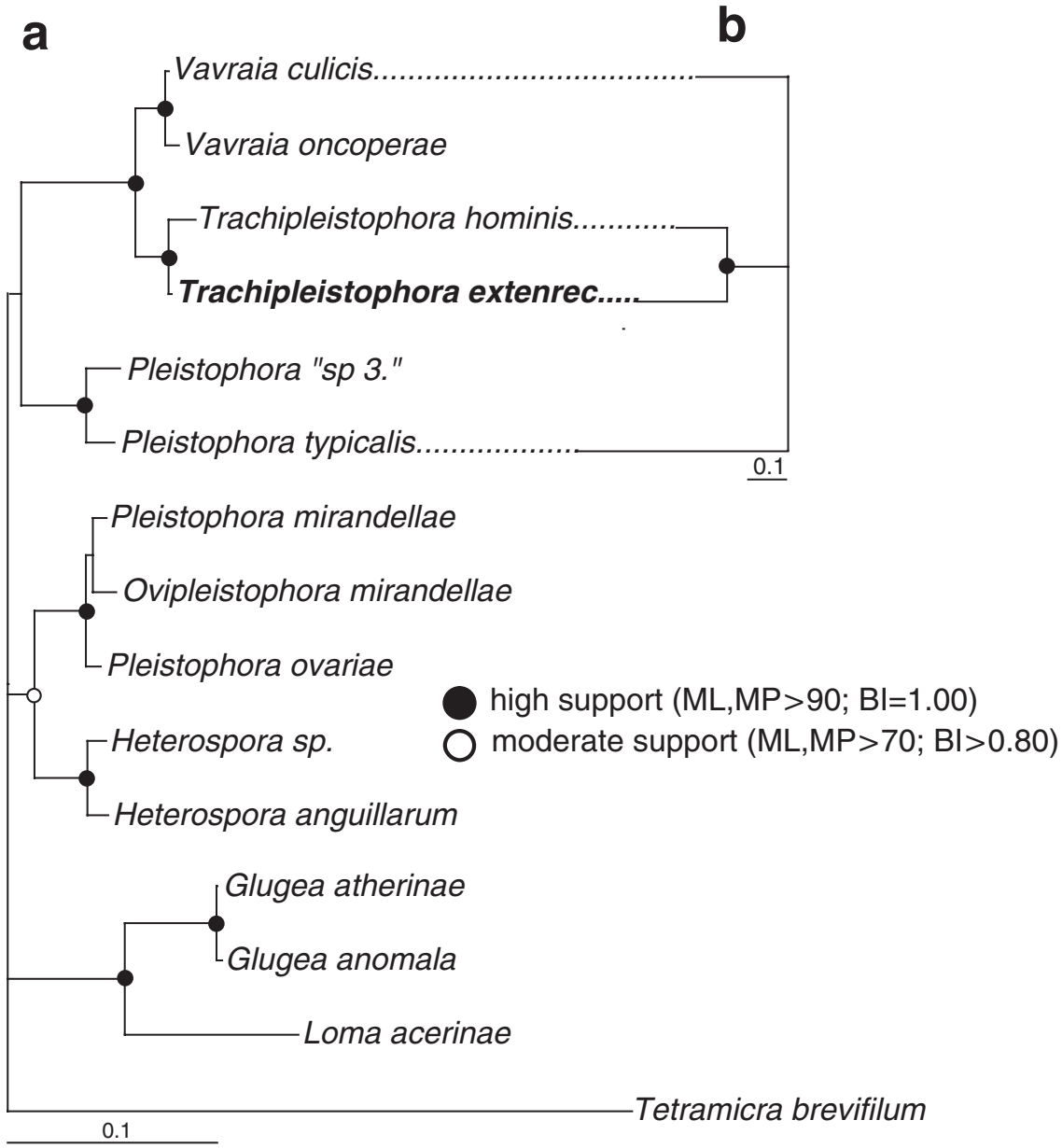

Fig. **39.** Strict consensus maximum likelihood g-corrected phylogenetic tree of microsporidians as revealed by analysis of (**A**) the small subunit (SSU) rRNA gene sequence and (**B**) sequence of the D-F region of the RNA polymerase subunit II gene constructed from all Ts:Tv settings and methods used (12 trees + 12 trees). Branch lengths, tree, and model parameters below applies to Ts:Tv set to 1:3. The SSU rRNA tree was constructed from 1,174 characters (195 parsimony informative) using GTR+A8+I model of evolution as implemented in Phyml 2.4.4. All parameters were estimated from the dataset (A: loglk = −4539.22717, á = 0.226, PINVAR = 0.000; B: loglk = −1935.96343, á = 2.129, PINVAR = 0.145). Symbols on the base of the nodes represents statistical support (see Materials and Methods for details).

```
                                562              579(563)
Vavraia culicis     TCGGTGATAGGA----------------CAAGGAC
Pl. typicalis       TGAGTGGTAGTA----------------CGTGTAT
Tr. hominis         ATGGTTATAGTGGTGAAGATAACATTAACAAGGGT
Tr. extenrec        ATGATGGTATTGGTGCGGGTGTTGTAATCAACTAT
```

Fig. **40.** Alignment of the nucleotide sequences of part of the RNA polymerase subunit II (RBP1) gene containing an insertion characteristic for both members of the genus *Trachipleistophora*.

Table **1.** Some host and structural characters of microsporida of the *Vavraia-Trachipleistophora* clade.

Species	Host(s)	Sporont	Sporont division	Spore size (μm)	Polar tube coils (thick/thin)	RNA polymerase subunit II motive
T. extenrec n. sp. (1)	Mammalia: Tenrecidae; Muridae	Multinucleate	Plasmotomy	4.7 × 2.8	15–16/0 two rows	Insert present
T. hominis (2)	Mammalia: Hominidae; Muridae	Uninucleate (2); rarely Multinucleate (1)	Binary fissions (2); Plasmotomy (1)	4.0 × 2.4	7–8/3	Insert present
T. anthropophtera (3)	Mammalia: Hominidae	Uninucleate	Binary fissions	3.7 × 2.0 (a) 2.2 × 2.5 (b)	7/2 (a) 4–5/0 (b)	?
V. culicis (4)	Diptera: Culicidae (4, 6) Lepidoptera (6)	Multinucleate	Plasmotomy rosette division	5.6 × 3.0 (1) 7.1 × 4.5 (7) 5.4 × 3.2 (14)	12 (8–9/3–4) (1) 15 (11/4) (5) 12–13 (8–9/3–4) (7)	Not insert
V. oncoperae (8)	Lepidoptera: Hepialidae	Multinucleate	Plasmotomy rosette division	5.0 × 2.6	10–15/?	?
V. sp. (9)	Diptera: Ceratopogonidae	Multinucleate	Rosette division	3.8–2.2	5–6/5–6	?
V. parastacida (10)	Crustacea: Decapoda	Multinucleate	Multiple fission	5.5 × 2.6	9–11/0	?
V. holocentropi (11)	Trichoptera: Polycentropidae	Multinucleate	Plasmodium fragmentation	9.8–6.0 × 2.0–2.1 (c) 2.2–3.0 × 1.7–1.8 (d)	6–8/3–4 (c) 3–4/3–4 (d)	?
V. mediterranica (12)	Crustacea: Decapoda	Multinucleate	Multiple division	2.3–1.4	(5)–6–7 ''anisofilar''	?
V. lutzomyiae (13)	Diptera Psychodidae	Multinucleate	Multiple division	6.1 × 3.1.	8–9/3–4	?

(1) This paper; (2) Hollister et al. (1996); (3) Vávra et al. (1998); (4) Weiser and Coluzzi (1972), Weiser (1977); (5) Canning and Hazard (1982); (6) Becnel et al. (2005); (7) Diarra and Toguebaye 1991; (8) Malone, Wigley, and Dhana (1987); (9) Atkinson (1990); (10) Langdon (1991); (11) Larsson (1986); (12) Azevedo (2001); (13) Matos, Mendonça, and Azevedo (2006); (14) Fukuda, Willis, and Barnard (1997); (a) sporogony type I; (b) sporogony type II; (c) macrospores; and (d) microspores.

Note: According to Larsson (1986) *Vavraia cyclocypris* (Voronin and Melnikova 1984) does not belong to the genus *Vavraia*.

with International Code of Zoological Nomenclature (Article 31.1) as a noun in apposition.

Molecular sequences. SSU rRNA: GenBank Accession number DQ403816 and RPB1: GenBank accession number DQ442657.

Type material. Type slides and specimens (paraffin or plastic resin blocks) are held at the Department of Parasitology, University of Veterinary and Pharmaceutical Sciences Brno, Czech Republic. Spores frozen in liquid N_2 are deposited at the Department of Parasitology, Faculty of Science Charles University, Prague, Czech Republic.

ACKNOWLEDGMENTS

We acknowledge the help of Barbora Šebestová in early stages of this project. Marie Flašková is thanked for preparing tissue samples for histology and Marie Váchová for caring of experimental animals. Technical support was provided by the Laboratory of Electron Microscopy of the Institute of Parasitology and its head Jana Nebesářová. The skilful help of Eva Kirchmannová and Marie Vancová in processing electron microscopy samples is gratefully acknowledged. This study was supported by Grant Agency of the Czech Academy of Sciences (524/03/H133), Research Project of the Institute of Parasitology, ASCR (Z60220518) and by Ministry of Education of the Czech Republic (6007665801).

LITERATURE CITED

Atkinson, C. T. 1990. Fine structure and sporogonic development of a *Vavraia* sp. (Microsporidia: Pleistophoridae) in the biting midge *Culicoides edeni* (Diptera: Ceratopogonidae). *J. Invertebr. Pathol.*, **55**:105–111.

Azevedo, C. 2001. Ultrastructural aspects of a new species, *Vavraia mediterranica* (Microsporidia, Pleistophoridae), parasite of the French mediterranean shrimp, *Crangon crangon* (Crustacea, Decapoda). *J. Invertebr. Pathol.*, **78**:194–200.

Becnel, J. J., White, S. E. & Shapiro, A. M. 2005. Review of microsporidia–mosquito relationships: from the simple to the complex. *Folia Parasitol.*, **52**:41–50.

Cali, A. & Takvorian, P. M. 2003. Ultrastructure and development of *Pleistophora ronneafiei* n. Sp., a microsporidium (Protista) in the skeletal muscle of an immune-compromised individual. *J. Eukaryot. Microbiol.*, **50**:77–85.

Canning, E. U. & Hazard, E. I. 1982. Genus *Pleistophora* Gurley, 1893—an assemblage of at least 3 genera. *J. Protozool.*, **29**:39–49.

Canning, E. U. & Lom, J. 1986. The Microsporidia of Vertebrates. Academic Press, London, UK. 289 p.

Canning, E. U. & Vávra, J. 2000. Phylum microsporidia balbiani, 1882. *In*: Lee, J. J., Leedale, G. F. & Bradbury, P. (ed.), The Illustrated Guide to the Protozoa. 2nd ed., **Vol. 1**. Society of Protozoologists, Lawrence, KS, 39–126.

Canning, E. U., Killick-Kendrick, R. & Killick-Kendrick, M. 1991. A new microsporidian parasite, *Flabelliforma montana* N. G., N. Sp., infecting *Phlebotomus ariasi* (Diptera, Psychodidae) in France. *J. Invertebr. Pathol.*, **57**:71–81.

Castresana, J. 2000. Selection of conserved blocks from multiple alignments for their use in phylogenetic analysis. *Mol. Biol. Evol.*, **17**:540–552.

Cheney, S. A., Lafranchi-Tristem, N. J. & Canning, E. U. 2000. Microsporidia based on small subunit ribosomal DNA sequences and implications for the source of *Trachipleistophora hominis* infections. *J. Eukaryot. Microbiol.*, **47**:280–287.

Cheney, S. A., Lafranchi-Tristem, N. J., Bourges, D. & Canning, E. U. 2001. Relationships of microsporidian genera, with emphasis on the polysporous genera, revealed by sequences of the largest sub-

unit of RNA polymerase II (RPB1). *J. Eukaryot. Microbiol.*, **48**: 111–117.

Diarra, K. & Toguebaye, B. S. 1991. On the development cycle and ultrastructure of *Vavraia culicis* Weiser, 1947 (*Microsporidia, Pleistophoridae*) with comments on the taxonomy of the genus *Vavraia* Weiser, 1977. *Eur. J. Protistol.*, **27**:134–140.

Didier, E. S., Didier, P. J., Snowden, K. F. & Shadduck, J. A. 2000. Microsporidiosis in mammals. *Microb. Infect.*, **2**:709–720.

Fast, N. M., Logsdon, J. M. & Doolittle, W. F. 1999. Phylogenetic analysis of the TATA box binding protein (TBP) gene from *Nosema locustae*: evidence for a microsporidia–fungi relationship and spliceosomal intron loss. *Mol. Biol. Evol.*, **16**:1415–1419.

Fukuda, T., Willis, O. R. & Barnard, D. R. 1997. Parasites of the Asian tiger mosquito and other container-inhabiting mosquitoes (Diptera: Culicidae) in northcentral Florida. *J. Med. Entomol.*, **34**:226–233.

Guindon, S. & Gascuel, O. 2003. Simple, fast and accurate algorithm to estimate large phylogenies by maximal likelihood. *Syst. Biol.*, **52**: 696–704.

Hall, T. A. 1999. Bioedit: a user-friendly biological sequence alignment editor and analysis program for Windows 95/98/NT. *Nucl. Acids Symp. Ser.*, **41**:95–98.

Hirt, R. P., Logsdon, J. M., Healy, B., Dorey, M. W., Doolittle, W. F. & Embley, T. M. 1999. Microsporidia are related to Fungi: evidence from the largest subunit of RNA polymerase II and other proteins. *Proc. Natl. Acad. Sci. USA*, **96**:580–585.

Hollister, W. S., Canning, E. U., Weidner, E., Field, A. S., Kench, J. & Marriott, D. J. 1996. Development and ultrastructure of *Trachipleistophora hominis* N. G., N. Sp. after in vitro isolation from an AIDS patient and inoculation into athymic mice. *Parasitology*, **112**:143–154.

Huelsenbeck, J. P. & Ronquist, F. 2001. MrBayes: Bayesian inference of phylogenetic trees. *Bioinformatics*, **17**:754–755.

Juarez, S. I., Putaporntip, C., Jongwutiwes, S., Ichinose, A., Yanagi, T. & Kanbara, H. 2005. In vitro cultivation and electron microscopy characterization of *Trachipleistophora anthropophthera* isolated from cornea of an AIDS patient. *J. Eukaryot. Microbiol.*, **52**:179–190.

Keeling, P. J., Luker, M. A. & Palmer, J. D. 2000. Evidence from beta-tubulin phylogeny that microsporidia evolved from within the fungi. *Mol. Biol. Evol.*, **17**:23–31.

Koudela, B., Vávra, J. & Canning, E. U. 2004. Experimental infection of severe combined immunodeficient (SCID) mice with the human microsporidian *Trachipleistophora hominis*. *Parasitology*, **128**:377–384.

Koudela, B., Visvesvara, G. S., Moura, H. & Vávra, J. 2001. The human isolate of *Brachiola algerae* (Phylum Microspora): development in SCID mice and description of its fine structure features. *Parasitology*, **123**:153–162.

Langdon, J. S. 1991. Description of *Vavraia parastacida* Sp. Nov. (Microspora: Pleistophoridae) from marron *Cherax tenuimanus* (Smith), (Decapoda: Parastacidae). *J. Fish Dis.*, **14**:619–629.

Larsson, J. I. R. 1986. Ultrastructural study and description of *Vavraia holocentropi* n. Sp. (Microspora, Pleistophoridae), a parasite of larvae of the caddisfly *Holocentropus dubius* (Trichoptera, Polycentropidae). *Protistologica*, **22**:441–452.

Lom, J. & Nilsen, F. 2003. Fish microsporidia: fine structural diversity and phylogeny. *Int. J. Parasitol.*, **33**:107–127.

Malone, L. A., Wigley, P. J. & Dhana, S. D. 1987. Identity of a microsporidium from three New Zealand pasture insects: *Costelytra zealandica* (Coleoptera: Scarabeidae), *Wiseana* spp. (Lepidoptera, Hepialidae), and *Listronotus bonariensis* (Coleoptera: Curculionidae). *J. Invertebr. Pathol.*, **49**:135–144.

Maslov, D. A., Lukeš, J., Jirkù, M. & Simpson, L. 1996. Phylogeny of trypanosomes as inferred from the small and large subunit rRNAs: implications for the evolution of parasitism in the trypanosomatid protozoa. *Mol. Biochem. Parasitol.*, **75**:197–205.

Mathis, A., Weber, R. & Deplazes, P. 2005. Zoonotic potential of the Microsporidia. *Clin. Microbiol. Rev.*, **18**:423–445.

Matos, E., Mendonça, I. & Azevedo, C. 2006. *Vavraia lutzomyiae* N. Sp. (Phylum Microspora) infecting the sandfly *Lutzomyia longipalpis* (Psychodidae, Plebotominae), a vector of human visceral leishmaniasis. *Eur. J. Protistol.*, **42**:21–28.

Posada, D. & Crandall, K. A. 1998. Modeltest: testing the model of DNA substitution. *Bioinformatics*, **14**:817–818.

Swofford, D. L. 2002. PAUP*: Phylogenetic Analysis Using Parsimony (and Other Methods). Sinauer Associates, Sunderland.

Thompson, J. D., Gibson, T. J., Plewniak, F., Jeanmougin, F. & Higgins, D. G. 1997. The clustalx windows interface: flexible strategies for multiple sequence alignment aided by quality analysis tools. *Nucleic Acid Res.*, **24**:4876–4882.

Vávra, J. & Larsson, R. 1999. Structure of the Microsporidia. *In*: Wittner, M. & Weiss, L. (ed.), The Microsporidia and Microsporidiosis. ASM Press, Washington, DC. p. 7–84.

Vávra, J. & Maddox, J. V. 1976. Methods in Microsporidiology. *In*: Bulla, L. A. & Cheng, T. C. Jr. (ed.), Comparative Pathobiology of the Microsporidia. Plenum Press, New York. p. 341–365.

Vávra, J., Dahbiová, R., Hollister, W. S. & Canning, E. U. 1993. Staining of microsporidian spores by optical brighteners with remarks on the use of brighteners for the diagnosis of AIDS associated human microsporidioses. *Folia Parasitol.*, **40**:267–272.

Vávra, J., Yachnis, A. T., Shadduck, J. A. & Orenstein, J. M. 1998. Microsporidia of the genus *Trachipleistophora*-causative agents of human microsporidiosis: description of *Trachipleistophora anthropophthera* n. sp. (Protozoa: Microsporidia). *J. Eukaryot. Microbiol.*, **45**:273–283.

Voronin, V. N. & Melnikova, O. Y. 1984. *Vavraia cyclocypris* Sp. N., the first find of a microsporidian parasite from Ostracoda (Crustacea). *Parazitologiya*, **18**:482–484.

Vossbrinck, C. R. & Debrunner-Vossbrinck, B. A. 2005. Molecular phylogeny of the Microsporidia: ecological, ultrastructural and taxonomic considerations. *Folia Parasitol.*, **52**:131–142.

Vossbrinck, C. R., Andreadis, T. G. & Debrunner-Vossbrinck, B. A. 1998. Verification of intermediate hosts in the life cycles of Microsporidia by small subunit rDNA sequencing. *J. Eukaryot. Microbiol.*, **45**: 290–292.

Weidner, E., Canning, E. U. & Hollister, W. S. 1997. The plaque matrix (PQM) and tubules at the surface of intramuscular parasite, *Trachipleistophora hominis*. *J. Eukaryot. Microbiol.*, **44**:359–365.

Weiser, J. 1977. Contribution to the classification of the Microsporidia. *Věst. Čsl. Spol. Zool.*, **41**:308–320.

Weiser, J. & Coluzzi, M. 1972. The microsporidian *Pleistophora culicis* Weiser (1946) in different mosquito hosts. *Folia Parasitol.*, **19**:197–202.

Received: 03/13/06, 06/01/06; accepted: 06/07/06